Journal of Electron Spectroscopy and Related Phenomena 257 (2022) 146901

Contents lists available at ScienceDirect

Journal of Electron Spectroscopy and Related Phenomena

journal homepage: www.elsevier.com/locate/elspec

# Short-wavelength four wave mixing experiments using single and two-color schemes at FERMI

F. Bencivenga [a,*], F. Capotondi [a], L. Foglia [a], A. Gessini [a], G. Kurdi [a], I. Lopez-Quintas [b], C. Masciovecchio [a], M. Kiskinova [a], R. Mincigrucci [a], D. Naumenko [a], I. Nikolov [a], E. Pedersoli [a], A. Simoncig [a]

[a] Elettra-Sincrotrone Trieste S.C.p.A., S.S. 14 km 163, 5 in Area Science Park, I-34149 Basovizza, Trieste, Italy
[b] University of Salamanca, Patio de Escuelas, 1, 37008 Salamanca, Castilla y León, Spain

ARTICLE INFO

*Keywords:*
X-rays
Free electron lasers
Four wave mixing
Transient grating

ABSTRACT

The development of ultra-bright extreme ultraviolet (EUV) and X-ray free electron laser (FEL) sources has enabled the extension of wave-mixing approaches into the short wavelength regime. Such a class of experiments relies upon nonlinear interactions among multiple light pulses offering a unique tool for exploring the dynamics of ultrafast processes and correlations between selected excitations at relevant length and time scales adding elemental and site selectivity as well. Besides the availability of a suitable photon source, the implementation of wave mixing methodology requires efforts in developing the instrumental set-up. We have realized at the FERMI FEL two dedicated set-ups to handle multiple FEL beams with preselected parameters in a non-collinear fashion and control their interaction sequence at the target. These unique apparatuses, combined with the exceptional characteristics of the seeded FERMI FEL, have allowed us to make the first steps into this field and further advances are foreseen in the near future.

## 1. Introduction

The nonlinear optical response (wave-mixing) occurs when multiple photon pulses with adequate brightness are brought to interact with a sample. The capability to control the photon parameters of the input pulses turns into a paramount opportunity to select specific interactions for probing the properties of the sample under investigation. The wide range of possibilities offered by the wave-mixing approaches has boosted a manifold of optical methods, applied nowadays in diverse fields for disparate purposes. The combination of wave-mixing capabilities with the chemical selectivity of EUV and X-ray photons can disclose totally new classes of experiments, where dynamic processes and correlations between selected atoms in a sample can be monitored on fs and nm time and length scales [1–4].

Though theoretically evaluated in great details [1–3], the practical realization of wave-mixing experiments in the EUV and x-ray regime has become possible only recently, thanks to the advent of short wave length FELs with unprecedented brightness and coherence. However, the realization of the wave-mixing experimental approach is still at an embryonal status and most of the pioneering experiments have been limited to demonstrate that a certain process (e.g. coherent emission [5,6], nonlinear Compton scattering [7], second harmonic generation [8–10], optical/x-ray wave-mixing [11], etc.) can be observed under given conditions, but none of these processes has been exploited to get information on the sample dynamics. Additionally, most of these experiments were focused on second order processes, which inherently have a range of applicability much narrower (by reasons of sample symmetry and number of interactions) than the third order processes, also known as four wave mixing (FWM) [1–4,12]. FWM comprises processes already commonly exploited in the table-top optical lasers experiments, such as stimulated Raman/Brillouin scattering, transient grating, optical Kerr effect, parametric conversion, phase conjugate imaging, 2D spectroscopy, etc.

Another lesson that can be learned from the optical experiments is the crucial role of handling and manipulating multiple input pulses that cannot trivially be implemented in EUV/x-ray instruments. These constrains, together with the limited access to the short wavelength FELs, are the main reason for the slow progress in experimental approaches to nonlinear EUV/x-ray optics. In this context it is worth noting how the use of more complex setups, involving third order processes and non-

* Corresponding author.
*E-mail address:* filippo.bencivenga@elettra.eu (F. Bencivenga).

https://doi.org/10.1016/j.elspec.2019.146901
Received 2 June 2019; Received in revised form 7 October 2019; Accepted 21 October 2019
Available online 31 October 2019

collinear beams in the so-called transient grating (TG) geometry [13–18], has allowed obtaining much better results providing more details about the sample response, such as time dependence and the spectral content of the EUV nonlinear processes [15–22]. The combination of optical TGs and EUV/x-ray pulses in FWM experiments was firstly exploited for monitoring the dynamics of surface deformations with unprecedented sensitivity [17]. This approach was successfully used in other fields, such as the study of electron-phonon coupling in semiconductors with atomic-selectivity [18] and ultrafast spectroscopy of atoms and molecules [15,16]. In all these cases, the dynamical response was detected relatively easy and detailed information on the time-dependent signal (e.g. the spectral content) was determined. However, the aforementioned experiments are based on table-top high-harmonic generation sources, which are not bright enough to generate FWM signals stimulated by EUV/x-ray pulses.

Ultrabright and fully coherent short wavelength FEL sources have opened the unique opportunity to use EUV pulses for generating TGs and follow their time evolution [20–22]. This has been a key step towards the development of the x-ray FWM approach envisioned by the theoreticians [1–3] that permits to drive excitations at nanoscale wavelengths [4,23,24], fully inaccessible by optical TGs (whose minimum spatial periodicity is half the wavelength of the generating pulses). The demonstration of EUV TGs has become possible thanks to realization of two special setups [20,25–27], which were purposely developed and implemented at the FERMI FEL facility operated at Elettra-Sincrotrone Trieste [28,29]. These setups are able to generate multiple FEL pulses (with some capabilities to select the wavelength of each input pulse), control their relative time delays and recombine them at the sample in a non-collinear geometry.

The designed and assembled FEL-based FWM setups, similar to table-top analogues [30], have definitely been a success. Here we briefly describe these setups and outline the on-going upgrades towards two complementary directions, i.e.: (i) improving the optically probed EUV TG approach (limited to relatively long TG wavelength) by implementing solutions already used in optical FWM and exploiting the multi-pulse/multi-color modes of FERMI with focus on ultrafast electron dynamics, and (ii) pushing the TG wavelength into the few nm regime using a third FEL pulse to monitor the dynamics stimulated by the nanoscale TG with focus on nanoscale transport processes, lattice and magnetic dynamics. The latter task resulted in the observation of a FWM signal exclusively stimulated by EUV pulses [31] and, more recently, in the determination of the time-dependent response at TG spatial periodicity as short as 28 nm [24], i.e. well beyond the optical domain. The developments of the setup based on the optical probing of the EUV TG have led to (i) the introduction of another variable in the experiment, that is the time delay (coherence time) between the FEL pulses that generate the EUV TG [27] and (ii) the first observation of a FWM signal stimulated by FEL pulses at different wavelengths [32,33].

## 2. FWM experiments based on a TG scheme

The magnitude of the (n+1)-wave-mixing response is proportional to the $n^{th}$-order nonlinear susceptibility, which is characterized by an unfavorable scaling vs the photon frequencies of the input beams that, however, is expected to be mitigated by the exploitation of core resonances [1–4,9,10,34]. On one hand, this situation makes low brightness EUV/x-ray sources unable to generate a wave-mixing signal without the assistance of one or more optical pulses. On the other hand, it highlights the great advantage of the background-free conditions, easily achievable in TG-based experiments, where two pump pulses with wave vectors (momentum) $k_1$ and $k_2$ overlap on the sample at an angle $\theta$ to generate an interference standing wave that acts as a diffraction grating for the "probe" pulse. The diffraction of the probe beam at wavelength $\lambda_{pr}$ from this interference pattern, called TG (Fig. 1a) is given by the grating equation:

$$L_{TG}\,[\sin(\theta_{in}) - \sin(\theta_{out,m})] = m\,\lambda_{pr}, \quad (1)$$

where $\theta_{in}$ and $\theta_{out}$ are the angle of incidence of the probe into the TG and the emission angle of the signal beam, respectively, m is an integer and $L_{TG}$ is the spatial periodicity of the TG, which is given by:

$$L_{TG} = \lambda_{ex}/2\sin(2\theta/2), \quad (2)$$

where $\lambda_{ex}$ and $2\theta$ are the wavelength and crossing angle of the pulses that generate the TG, respectively. Eq. 1 is valid for so-called “thin

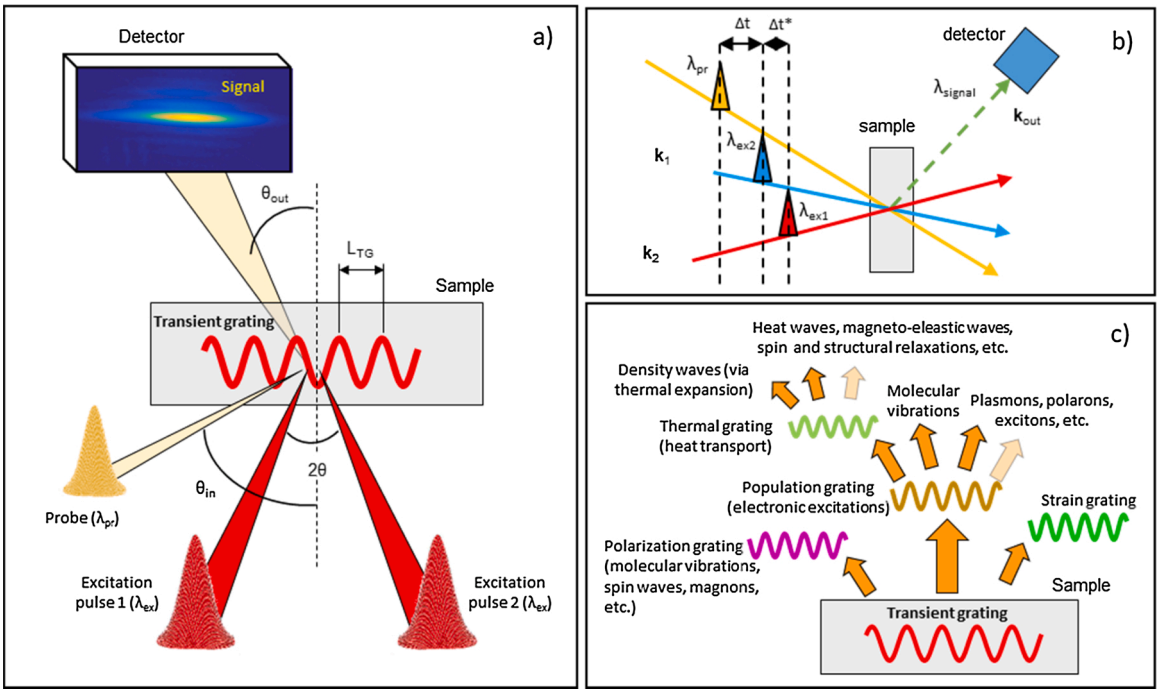


**Fig. 1. a)** Schematic description of a TG FWM experiment. **b)** Geometry and time separation of the four pulses (excitation 1 and 2, probe, signal) involved in the FWM. **c)** Some dynamical processes that can be accessed by TG experiments.

grating" conditions [35,36], which are typically fulfilled in EUV TG experiments with optical probing, because of the short absorption length of EUV excitation pulses and the relatively large values of $\lambda_{pr}$ and $L_{TG}$. In the case of EUV probing and small $L_{TG}$'s the "volume grating" conditions are met and a tangible diffraction can be observed only when $\theta_{out} = -\theta_{in}$ (Bragg diffraction). In the frame of nonlinear optics the diffraction of the probe beam from the TG can be regarded as a "phase matching" process, that is the coherent addition of the signal fields radiated from different sample locations along specific directions [12,37]. These specific directions are determined by the experimental geometry and, in non-collinear schemes, can be chosen to be vastly different from any input beam directions. Furthermore, the coherent addition causes an increase in the magnitude of the signal beam with the square of the elementary emitters within the coherence volume of the process (the number of grating lines in the case of TG). The directionality and the coherent signal generation process can result in a dominant nonlinear signal in such specific and pre-determined directions.

The exploitation of the TG scheme for achieving background free conditions is a winning strategy for developing EUV/x-ray nonlinear optics [15–22], since is allows reliable detection of weak nonlinear signals. Our EUV TG setups (Fig. 1b) are based on the use pump and probe beam parameters that have allowed us to carry out a more general FWM experiment. For instance, the time delay between the excitation pulses (coherence time, $\Delta t_c$) is naturally controllable and can be used in combination with the probe's delay ($\Delta t$) to perform 2D-measurements, while multiple EUV excitation wavelengths ($\lambda_{ex1}$, $\lambda_{ex2}$) can be delivered by the FERMI FEL [32,38,39] and used for coherent Raman scattering experiments. All this makes TG approach an ideal platform for developing the more universal x-ray FWM methodology.

It is apparent that in the TG FWM approach the periodicity of the created standing waves ($L_{TG}$) that determines the spatial resolution can be varied selecting the light wavelengths and crossing angle. The advent of FELs opening the opportunity to use shorter EUV and hard X-ray light have overcome the limitations of optical TG experiments (see Eq. 2) and today we can access a broad class of dynamical processes at the nanoscale matching selectively the distances corresponding to the excitations events of interest for investigation (some of them are sketched in Fig. 1c). For example, the possibility to generate nm-sized TGs and probe their dynamical response is of great relevance for exploring transport phenomena and structural dynamics at the nanoscale [40–45]. Further on, by tuning the pump and/or probe pulses wavelength to selected core electron transitions adds chemical and site specific information and can be applied for studies of charge and spin dynamics. The wavelength tunability allows following the electron dynamics as a function of EUV/X-ray absorption process and accessing the dependence of de-excitation processes on the electron energy and charge carrier density. However, one should also take into account some limitations that vary with the material under investigation and experimental conditions, such as (i) the differences in the probing depths when using pump wavelengths below and above the core electron edges; (ii) the occurrence of more than one thermalization process in the same instant and temporal overlap of excitation-thermalization processes [33]; (iii) the length of the pulses that can be within the time scale of core-hole lifetime; (iv) the precise phase control of FEL pulses etc.

## 3. Experimental setups

We realized two distinct EUV FWM setups at the FERMI FEL facility [26], sketched in Fig. 2. Both are based on the capability of generating EUV TGs. The first one in Fig. 2a) is mini-TIMER that relies upon optical probing that imposes a limit on the accessible $L_{TG}$ range to $\geq$ 200 nm. However, it allows exploiting the tunability and most of the available multi-pulse/multi-color options of the FERMI FEL. The second in Fig. 2b) is EIS-TIMER that offers a EUV probing option, which in principle allows pushing $L_{TG}$ down to the single digit nm regime, but at the price of less flexibilities compared to the first setup.

The natural scientific applications of EIS-TIMER target investigations of nanoscale properties of matter [23]. Among them, we mark ultrafast spin and thermal transport over 10's of nm scale. The mechanisms governing the ultrafast spin phenomenon are highly disputed in the current literature [45–48], but there is an undoubtable consensus in considering this process as the key to addressing the fundamental limits

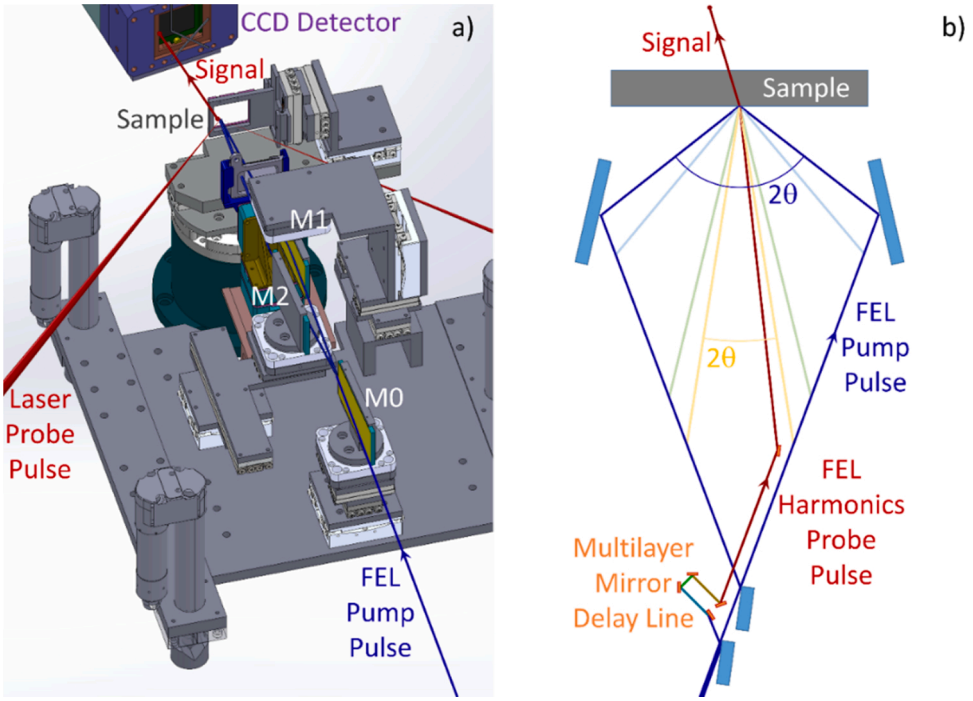


**Fig. 2.** EUV TG setups, both based on the splitting of a single FEL pulse by a mirror edge and the recombination on the sample with crossing angle 2θ. **a)** Mini-Timer is a compact system with small crossing angles that allow probing the TG with an optical laser. **b)** EIS-Timer uses large crossing angles to produce TG gratings with nm pitch, probed with higher FEL harmonics EUV photons.

of ultrafast spintronic devices. In this respect, for shedding light on the interplay of spin and heat at the nanoscale, we need to achieve full knowledge of the nanoscale thermal transport processes, when the characteristic size of the object is comparable with the mean free path of heat carrier phonons [42–44,49–51]. The nanoscale TG experimental approach is a perfect tool for addressing these topics [24,51,52]. Another important open question that can be addressed by nanoscale TGs is the long debated issue of thermal and vibrational anomalies of amorphous solids with respect to their crystalline counterpart [40, 53–56]. Indeed, despite the several different hypotheses made for describing this phenomenology, there is a common agreement that such a behavior relates to collective vibrational excitations (phonons) at a few nm wavelengths that are only partially accessible by the available experimental methods [23,40,57]. Vibrational excitations and transport processes are also relevant for micro/nano electro-mechanical systems (MEMS/NEMS), where mechanical and thermal dissipations at the nanoscale play a crucial role [58], and for the development of nanoscale devices able to harvest thermal and vibrational energy from the environment. In a nutshell, the capability to probe the thermoelastic response in the 1–100 nm range opens the route for tailoring nanoscale material properties and direct cutting edge technologies.

Core-hole resonances can be exploited by mini-TIMER, combining FEL pulses for selective atomic-site electron excitations and optical pulses, to monitor energy and charge transfer processes at the molecular scale.

Both EUV TG setups, mini-TIMER and EIS-TIMER, have been developed from the common concept, successfully tested in optical TG experiments [30], of splitting an FEL beam into two halves through the insertion of a plane mirror edge, working at grazing incidence as a wavefront-division beamsplitter. This guarantees the achromaticity of the system, providing beams whose directions do not depend on the FEL wavelength, $\omega_{FEL}$, and whose total intensity $(1+R(\omega_{FEL}))/2$, function of the mirror reflectivity $R(\omega_{FEL})$, is satisfactory on a wide range of $\omega_{FEL}$.

The main difference between the two setups is that mini-TIMER is a very simplified miniaturized version, with splitting and recombining mirrors operating at grazing incidence within a sole experimental chamber, where the beam is tailored by a Kirkpatrick-Baez (K-B) focusing system positioned before the splitting mirror and the created TG is probed with an optical beam, while EIS-TIMER is a large-scale multi-component system, with multiple focusing optics hosted in separate vacuum chambers, operating at wide incidence angle to provide TGs with specific periodicity down to the single digit nm size, that is probed by EUV FEL light.

**Mini-TIMER**, depicted in Fig. 2a, is an improved version of the first setup used for the demonstration of EUV FWM [20]. The split and recombine system consists of three planar C-coated mirrors ($70 \times 30$ mm$^2$) arranged in a parallelogram geometry, each mounted with two translational and two rotational degrees of freedom on the same $300 \times 200$ mm$^2$ kinematic plate of the DiProI end station vacuum chamber. The FEL beam is split by the edge of the first mirror M0 into a transmitted and a reflected half beam, respectively impinging on mirrors M1 and M2, 125 mm downstream the M0 edge, to be recombined on the sample placed 125 mm further downstream. For each mirror, X, Z, pitch and roll are precisely controlled by four encoded piezoelectric stages, enabling the system to be positioned in parallelograms with continuously tunable values of the crossing angle $2\theta$. A single K-B active optics system [59], located 1.2 m upstream the sample, permits to independently and reliably set the vertical and horizontal spot size at the sample in a broad range, from about 1 mm to a few 10's of μm.

Thanks to the wide footprints and grazing incidence of the beams on the mirrors, the reflectivity of the C coatings remains satisfactory for several days; when the mirrors undergo a local damage, fresh spots are made available to the FEL beam, varying the vertical position of the mini-TIMER kinematic plate by the three stepper motors. Still we lack precise quantitative evaluation of radiation damage since it strongly depends on the beam parameters that vary with different experiments. Our observation is that under typical operation conditions of Mini-Timer (i.e. pulse energy of 1–10 μJ, duration 50 fs, wavelength 12–30 nm and spot size 25 μ m$^2$) and the damage becomes noticeable after ~ 24 h of continuous measurements. In the case of EIS-TIMER the situation is much better since the footprint on the last (focusing) mirrors is much larger (~1000 μ m$^2$) so we have not noticed a significant drop in the mirror reflectivity even after 12 weeks of operation.

The TG dynamics are probed by an optical laser pulse of wavelength $\lambda_{pr}^{opt}$, coplanar with the FEL beams, impinging on the sample with an incidence $\theta_{in}^{opt}$ of about $45^\circ \pm 3^\circ$; the maximum signal is achieved in the TG phase matching condition, corresponding to the Bragg configuration, for $\sin(\theta)/\lambda_{FEL} = \sin(\theta_{in}^{opt})/\lambda_{pr}^{opt}$. Since the penetration depth in the sample is typically shorter for the FEL radiation than for the probe, the "thin grating" conditions are satisfied and a FWM signal can be generated out of phase matching [35,36].

Mini-TIMER is a small, simple, reliable, controlled and automatized system. Its main constrain is the accessible exchanged TG momentum $|\mathbf{k}|$ of the modes excited by the interference of the two pump beams, limited by the grazing condition of the θ angle and by the probe wavelength to a range $|\mathbf{k}| < 2|\mathbf{k}_{pr}^{opt}|$. Both the forward-diffracted FWM signal passing through transparent samples and back-reflected WFM signal can be detected simultaneously on two CCD detectors.

Taking advantage of the reliable positioning of the mini-TIMER configuration, an automatic procedure has been developed to introduce a controlled time delay between the two FEL beams and scan the delay value in a cross correlation measure, detecting the FWM signal to characterize pulse duration, temporal profile and coherence of the FEL pulses [27].

**EIS-TIMER**, depicted in Fig. 2b, aims at the exploration of FWM in the high-$|\mathbf{k}|$ regime [23], up to $\approx 1$ nm$^{-1}$; this requires the system to scale to the size of a full beamline, since each beam needs its own focusing mirror in a separate vacuum chamber as the last optical component before the sample. To achieve phase matching at the Bragg condition, the TG is probed by a third FEL pulse, with a wavevector, $\mathbf{k}^{pr}{}_{FEL}$, larger than $\mathbf{k}_{FEL}$ of the exciting pulses.

Each FERMI pulse is first split into two halves (pump and probe) by the edge of a gold plated plane mirror (≈15 m upstream the sample). The pump is further split into two beams, finally recombined on the sample by pairs of carbon or gold coated toroidal mirrors, which can be inserted in the beam path, spanning a fixed set of four crossing angles $2\theta = 18.4^\circ$, $27.6^\circ$, $79.0^\circ$ and $104.8^\circ$.

The probe pulse is sent into a delay line, composed of four multilayer mirrors, with reflectivity (for vertically polarized light) of 0.55@17.8 nm, 0.64@13.3 nm, 0.55@6.7 nm and 0.24@3.3 nm, that allows scanning the time delays Δt up to a few ns thanks to an active feedback stabilization [25]. The delayed probe is then focused and recombined on the sample, impinging at an angle $\theta_{pr} = 3.05^\circ$, $4.6^\circ$, $12.2^\circ$, $15.4^\circ$, by one of the four available carbon or $TiO_2$ coated toroidal mirrors. The delay line selects the probe wavelength $\lambda_{pr}$, usually the third harmonics of the main FEL wavelength $\lambda_{ex}$, since the condition $\lambda_{ex}/\lambda_{pr} = 3$ allows for a substantial angular separation between input and emitted beams and FERMI can work in conditions that provide a third harmonics contribution up to 5% of the total output.

The entire EIS-TIMER setup requires 12 focusing mirrors, bringing up some technical complexities, as for instance the use of 84 independent motors only for mirrors tuning.

## 4. EUV TG measurements

The development of our EUV TG setups has allowed for a substantial improvement in the quality of the data and for new types of measurements. Fig. 3 displays a comparison between data for diamond collected in 2015 using the first prototype of the mini-TIMER setup (red) and those recently obtained using the present upgraded version (black) (from Ref. [22]). The latter were collected using $\lambda_{ex} = 12.7$ nm and FEL fluence, F ~ 10 mJ/cm$^2$, while the former using $\lambda_{ex} = 26.1$ nm and F ~

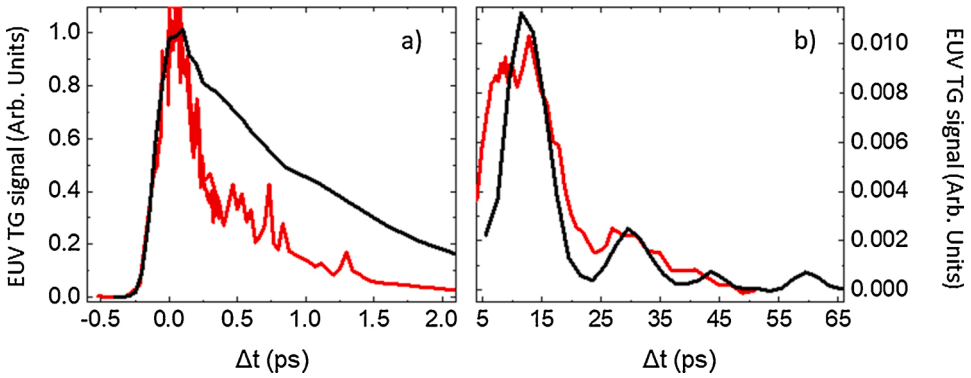


**Fig. 3.** EUV TG signal from diamond sample acquired with the prototype mini-TIMER setup (red lines) and with the improved setup (black lines; from Ref. [22]). (a) the initial signal decay: the different decay times are due to different excitation densities; (b) the beginning of the phonon modulations at longer time scales: the oscillation frequency is identical since the created $L_{TG}$ was the same in both experiments.

40 mJ/cm$^2$. In both cases we used $\theta_{in} = 45°$ and $\lambda_{pr} = 390$ nm, while the value of 2θ was adjusted according to Eq. 2 in order to set $L_{TG} \sim 280$ nm.

Both data sets show a fast rise of the EUV TG signal over a zero background level, the behavior expected in a typical TG experiment, where the signal "appears" in a background free direction, determined by the experimental geometry and chosen to be vastly different from the directions of the input beams (see, e.g. Fig. 1). In the EUV regime where the input wavelength is far from any core-edge, as in the present cases, the leading excitation channel is the "instantaneous" generation of hot electrons/holes in the valence/conduction band, which quickly (~ 10 fs) relax into a population of electron-hole pairs across the bandgap [60–62]. These initial dynamics cannot be monitored with the time duration of the employed pulses (i.e. 50–70 fs for the FEL and ~120 fs for the optical). On longer timescales, when some of the excitation energy is transferred to the lattice, the EUV TG introduces a spatial modulation of the lattice excitation process. Thus, the initial decay of the EUV TG signal can be ascribed to this dynamics. The observed decrease of the TG contrast directly reflects the changes of the refractive index at the probe's (optical) wavelength when the electronic excitations relax into the lattice becoming less pronounced for variations in the lattice parameters (e.g. temperature and density). The different decay time reported by the two dataset in Fig. 3(a) indicates that the electronic relaxation is faster for larger values of the excitation energy density, as previously observed for silicon nitride [21]. In this context it is worth mentioning that in addition to the larger value of F used for the measurements at 26.1 nm, the EUV absorption length at this wavelength ($L_{abs} \sim 26$ nm) is about 4 times shorter than that at $\lambda_{ex} = 12.7$ nm ($L_{abs} \sim 110$ nm). Besides such a difference in the decay time of the electronic excitation grating, one can appreciate how, for comparable accumulation time, the data collected in 2015 with the prototype setup are substantially noisier than the data acquired with the actual one. This improved signal quality allows for the reliable detection of fine details of the signal, such as the dynamics of density modulations (acoustic phonons) and thermal diffusion modes at the TG wavelength ($L_{TG}$), occurring at timescales much longer than the initial electronic decay [22]. In Fig. 3b one can appreciate how the contrast (~$10^3$) of the older data is barely sufficient to observe the onset of phonon oscillations, while in the new data (contrast ~$10^5$) these features are well defined; note that the oscillation frequency is the same because $L_{TG}$ is the identical in both experiments. A detailed discussion of these data, which at even longer Δt's show a beating pattern between bulk and surface phonons, can be found in ref. [22].

The general advantage of the background free conditions can be perceived by comparing the decay of the EUV TG signal and the transient variation of optical reflectivity (ΔR/R) obtained in a 'classical' FEL-pump/optical-probe experiment. From the results reported in Fig. 4, obtained from the same sample, it is evident the superior quality of the EUV TG data compared to the transient reflectivity one where the small

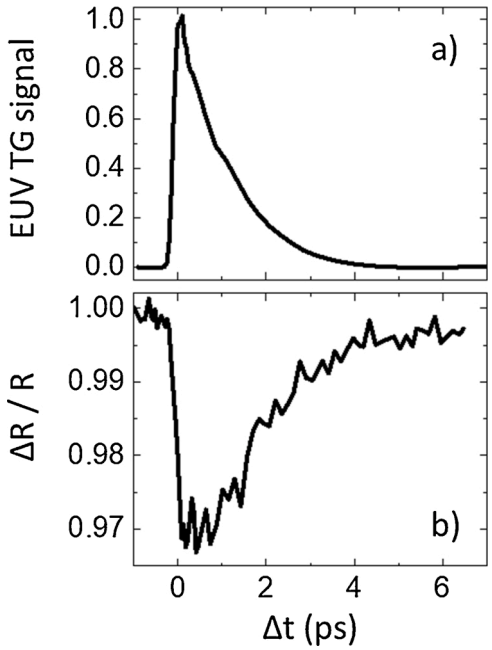


**Fig. 4. a)** Initial decay of the EUV TG signal from diamond acquired with the upgraded setup. **b)** Transient optical reflectivity data, collected using 'classical' FEL-pump/optical-probe conditions (see text).

time dependent variations should be monitored in the presence of large constant signal (i.e. the un-pumped optical reflectivity in the present case). It is apparent that signal details as fine as those shown in Fig. 3b are unlikely to be observable in classical transient reflectivity experiments. Finally, for the sake of completeness, we notify that the EUV TG signal is quadratic with respect to the FEL-induced variations of the optical refraction index while the ΔR/R one is linear, therefore in the transient reflectivity experiment a signal decay about twice longer than the EUV TG one is expected.

Fig. 5 shows EUV TG data from vitreous $SiO_2$ (i.e. the prototypical example of strong glasses) in a few ps timescale range that could contain information about the local vibrational dynamics of $SiO_2$ molecules, relevant for understanding the vibrational anomalies of disordered systems compared to their crystalline counterparts. The first results, obtained with the initial prototype setup (red), are compared to those, measured with the upgraded one with apparently better quality. The signal comprises for all exploited conditions a sharp 'electronic' peak at $\Delta t = 0$, basically consistent with the cross-correlation of FEL and optical input pulses, followed by a non-zero modulated signal indicating a clear

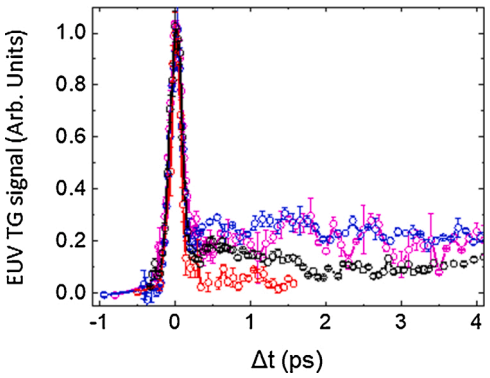


**Fig. 5.** EUV TG signal from vitreous $SiO_2$ corresponding to different experimental conditions: (red dots) F ~ 100 mJ/cm$^2$ and $\lambda_{ex}$ = 26.1 nm [20], (black dots) F ~ 10 mJ/cm$^2$ and $\lambda_{ex}$ = 32.6 nm, (magenta dots) F = 5 mJ/cm$^2$ and $\lambda_{ex}$ = 31 nm (blue dots), F = 2.5 mJ/cm$^2$ and $\lambda_{ex}$ = 21 nm.

dependence on $\lambda_{ex}$ and F. This behavior definitely hampers the straightforward interpretation of the EUV TG signal.

It should be notified that, while acoustic phonons and thermal relaxations, denoting thermoelastic response, have been observed for all studied samples under all experimental conditions (including reflection mode EUV TG [22], EUV probing and shorter $L_{TG}$'s [24]), molecular modes (Raman excitations) are more elusive. A clear evidence of Raman response in the EUV TG signal was reported for a BiGeO sample [22], where the dominant excitation mechanism is most likely displacive excitation of coherent phonons (DECP) [63]. However, DECP is unlikely to be effective in amorphous materials, like vitreous $SiO_2$, even though in some special cases DECP in amorphous systems wave was reported [64]. On the other hand, stimulated coherent Raman scattering mechanism, triggered by FEL pulses was recently observed in diamond [33], and found to be effective at higher F's but weaker than the thermoelastic response. These considerations suggest the need of a more comprehensive investigation of the local vibrational dynamics in vitreous $SiO_2$, which should include the dependence on both $\lambda_{ex}$ and F, other than that (still unexplored) on $L_{TG}$.

Another possibility offered by a multi-pulse FWM approach for getting information on the ultrafast sample dynamics is scanning the time delay ($\Delta t^*$) between the two FEL pulses generating the EUV TG (see Fig. 1b), while monitoring the transient diffraction signal by the optical probe. This approach has widely been used in optical spectroscopy, both for studying the temporal properties of the pulses (e.g. via TG FROG or self-diffraction [65,66]) and for obtaining information on the coherence properties of excited states (e.g. via three pulse photon echo or multidimensional spectroscopy [67,68]). This capability has already been implemented in the present version of mini-TIMER and was tested by verifying the time duration and coherence time of the FERMI FEL pulses [27]. Fig. 6a shows an example of such measurements, where the TG intensity was monitored as a function of the temporal overlap between the two crossing FEL pulses. The data show a nearly Gaussian profile (blue curve in Fig. 6a), which is consistent with a transform limited FEL pulse (i.e. a pulse with a constant phase for all spectral frequencies) with time duration of about 65 fs. This value is in good agreement with the value of 55 fs that can be obtained from the spectral line shape the FEL radiation (as displayed in Fig. 6b), within the assumption of a Gaussian profile. The discrepancy could be ascribed to several reasons, such as, for example, a residual chirp in the FEL pulses, deviations from Gaussian (time/frequency) profiles or the sample response. However, it is worth clarifying that without assumptions on the phase of the spectral components (such as the one made here, i.e. Fourier limited pulses), the interpretation of the EUV TG signal in terms of FEL pulse duration would need independent information about the spectral phases. However, these results shown here are not aimed at demonstrating a method for determining the FEL pulse duration but for highlighting the capability, inherent to the XTG approach, of controlling the additional temporal dimension ($\Delta t^*$).

In many FWM experiments, the capability to control the spectrum of the input pulses and to determine the spectrum of the output one are very relevant added values, which could peovide valuable information on sample dynamics. The implementation at mini-TIMER of a detection system capable to measure the signal spectrum as well as tailoring the probe pulse spectrum is relatively straightforward, because both the probe and the signal beams are in the optical regime. This task is much more complicated at EIS-TIMER, where all beams are in the EUV/soft x-ray range. However, the multi-pulse/multi-color options available at the FERMI FEL [38,39] could be profitably exploited for developing such more complex approach. Indeed, the first observation of a purely EUV FWM response was achieved by exploiting the multi-wavelength nature of the FEL emission, which allowed us to identify the FWM interactions between the fundamental FEL radiation and its harmonics [31].

While in many cases the presence of radiation different from the fundamental harmonic in the FEL spectrum is harmful, in FWM this could be an advantage. In fact, the relaxed phase matching conditions due to the short absorption length of the EUV radiation allows for the simultaneous observation of different FWM processes. For example, Fig. 7a shows the simultaneous occurrence of transient diffraction of the 2$^{nd}$ and 3$^{rd}$ harmonics of the FEL beam from an EUV TG generated on a 50 nm thick silicon nitride membrane by the fundamental radiation. Moreover, since both harmonics impinge onto the sample collinearly with one of the excitation pulses (see Fig. 7b), none of them is perfectly phase matched (i.e. they do not satisfy the Bragg scattering condition). In this context, the FEL source should be "detuned" in a way to produce a bunch of high harmonics of the seed laser, which can be spectrally located in the region around the 2$^{nd}$ and 3$^{rd}$ harmonics. This permits to

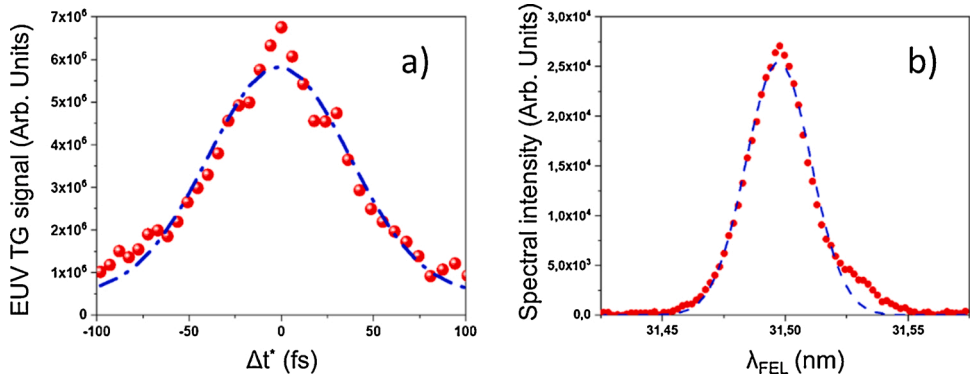


**Fig. 6. a)** EUV TG signal as a function of the time delay ($\Delta t^*$) between the two FEL pulses that generate the EUV TG. **b)** The corresponding FEL spectrum. Dashed lines in both panels are Gaussian functions.

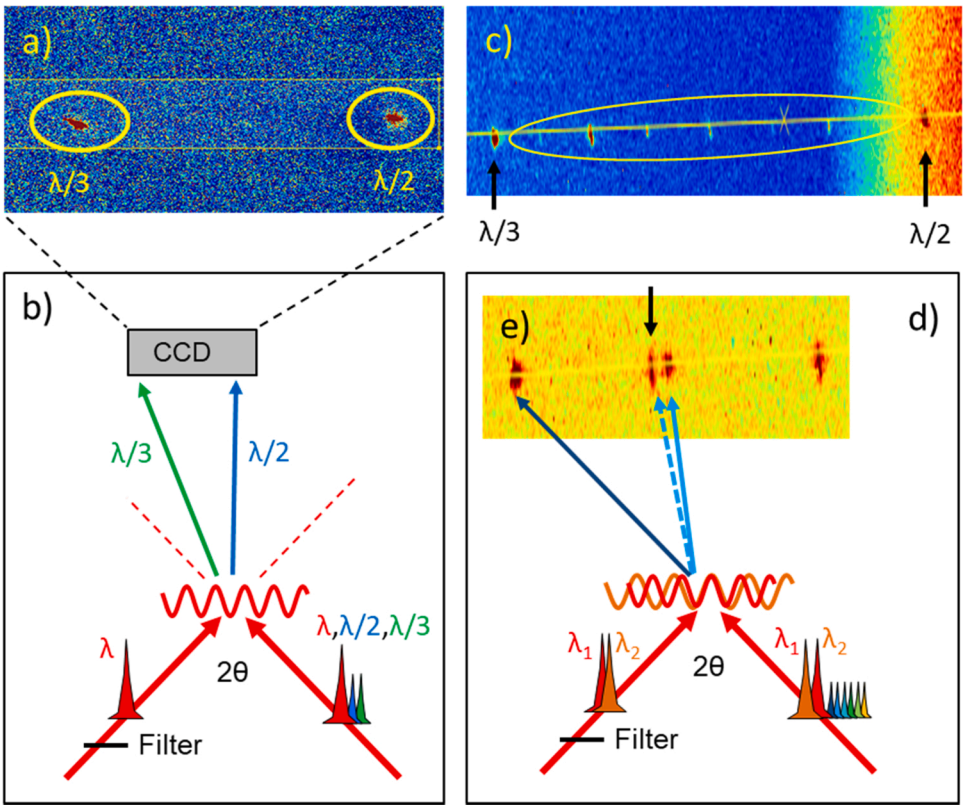


**Fig. 7. a)** Diffraction pattern of 2nd (λ/2) and 3rd (λ/3) FEL harmonics transiently scattered by an EUV TG generated on a silicon nitride membrane by the fundamental FEL radiation (λ = 28.9 nm). **b)** Sketch of an experiment where a Mg filter is used to cut the radiation with wavelength shorter than 25 nm (i.e. all the harmonics) from one excitation pulse. **c)** Same signal when the FEL emission also contains a substantial amount of high harmonics of the seed laser ($\lambda_n = \lambda_{seed}$ /n, with $\lambda_{seed} = 260$ nm and n ~ 15–30). **d)** Sketch of the situation where the FEL is tuned to emit two fundamental wavelengths ($\lambda_1 = 28.9$ nm and $\lambda_2 = 26$ nm). **e)** Some additional signals, whose origin is not yet understood, appear in the pattern, as the one indicated by the black down arrow.

observe simultaneously a set of FWM signals in an experiment like the one sketched in Fig. 7b, and these signals are spatially separated because of the dispersion due to the EUV TG (see Eq. 1). In Fig. 7c, we report an example of this condition, where two 28.9 nm excitation pulses (harmonic 9 of a 260 nm seed) generate the EUV TG, which is probed by a set of harmonics of the seed laser. Each probing harmonic generates its own spot on the CCD detector because of the TG dispersion. In the present case, the probe wavelengths span from 14.4 to 9.6 nm (i.e. from harmonic 18 to 27 of a 260 nm seed), demonstrating how this approach in principle allows the sample FWM response (with steps given by the photon frequency of the seed laser, i.e. ~ 3–5 eV) as a function of the EUV probe frequency in an extended range. The FERMI FEL can also be tuned for emitting more than one fundamental FEL frequency (see sketch in Fig. 7d), so that also multi-wavelength excitation is possible. Fig. 7e displays the signal observed when the FEL source was tuned in order to have a spectral content (for each FEL pulse), dominated by radiation at 26 and 28.9 nm (harmonics 10 and 9 of a 260 nm seed). Some additional spots appear sideways the ones shown in Fig. 7c, that might indicate a FWM interaction between the two exciting FEL wavelengths, though further studies and analysis are needed to describe this observation. It also is important to stress that none of the experimental configurations sketched in Fig. 7 permits to vary the time delay between the probing harmonics and the fundamental one within the same pulse, while one can in principle scan the delay between the crossed pulses coming from different sides. On the other hand, the FERMI FEL also offers the capability to set a controllable phase shift (i.e. a sub-fs delay) between the various harmonics [69]. Moreover, the possible exploitation of new concepts for generating soft x-ray FEL pulses, such as echo-enabled harmonic generation [4,70,71], should open new opportunities for more advanced multi-color/multi-wavelength operation modes. Whether the potential of this kind of multi-color FWM approach for studying ultrafast processes has still to be further explored, the main message arising from these initial observations is that the advantages of the non-collinear approach makes EUV TG a favored platform for developing FWM methods in the EUV and soft x-ray regime.

Further developments of the existing setups are ongoing, such as the Noncollinear Optical Parameter Amplifier (NOPA) that has been installed to expand the wavelength tunability and to increase the time resolution of the optical probe.

An extension of the available sample range to magnetic samples for studies of nanoscale magnetic dynamics or to liquid and gas phase is foreseen. The latter are very interesting in the context of the general development of EUV FWM, since they could both test the results of theoretical works promising to greatly help in interpreting the various signals/processes [1–3], and extend the range of existing experimental works with HHG [15,16].

## 5. Conclusions

We have provided an overview of our special instruments, based on the EUV TG scheme, realized at the FERMI FEL aiming at developing and exploiting the EUV/x-ray wave-mixing methodology. We described the recent implementations of the two setups, notifying the progresses made with respect to the first tests, and discussed the improvements to be accomplished in the near future. The driving force for the reported instrumental developments is the realization of two complementary apparatuses, one focused on nanoscale lattice dynamics and the other on ultrafast electronic dynamics. The capability to exploit EUV TGs for accessing nanoscale lattice dynamics has recently been demonstrated in experiments where an EUV probing pulse is used to follow the time evolution of vibrational and thermal modes at wavelengths as short as 28 nm [24]. The possibility to exploit multiple time-delays has been demonstrated in experiments focused on the characterization of coherent properties of the FEL emission, where we were able to resolve the few fs time structure featuring the FEL emission under different conditions [27]. The latter is a remarkable step forward towards 2D spectroscopies, where the atomic selectivity of the EUV pulses tuned at specific core resonances can be combined with the sensitivity of optical

pulses to valence-band excitations. The primary outlooks for these two complementary developments are (i) strengthening of the optical probe capabilities and multi-color operation for mini-TIMER and (ii) achieving spatial periodicity of the EUV TG down to the single-digit nm regime for EIS-TIMER. The latter task can be accomplished by realizing special multilayers coatings in order to exploit the short wavelength fraction of the spectral range accessible by the FERMI source. The optical probing at mini-TIMER has been implemented with a few fs NOPA device, the possibility to spectrally resolve the (optical) FWM signal is planned and an alternative setup, based on diffractive optical elements, is under evaluation for better handling multi-color FEL beams in a non-collinear FWM geometry. In a longer term, the capabilities developed at the two instruments could be eventually combined in order to make possible the realization of short-wavelength FWM experiments with much higher level of flexibility.

## Acknowledgments

We gratefully acknowledge Michele Svandrlik and all the FERMI team for their invaluable support. Authors acknowledge support from the European Research Council through the grant N. 202804-TIMER.

## References

[1] S. Tanaka, S. Mukamel, Phys. Rev. Lett. 89 (2002), 043001.
[2] S. Tanaka, V. Chernyak, S. Mukamel, Phys. Rev. A 63 (2001), 063405.
[3] D. Healion, Y. Zhang, J.D. Biggs, W. Hua, S. Mukamel, Struct. Dyn. 1 (2014) 14101.
[4] F. Bencivenga, S. Baroni, C. Carbone, M. Chergui, M.B.B. Danailov, G. De Ninno, M. Kiskinova, L. Raimondi, C. Svetina, C. Masciovecchio, New J. Phys. 15 (2013), 123023.
[5] N. Rohringer, D. Ryan, R.A. London, M. Purvis, F. Albert, J. Dunn, J.D. Bozek, C. Bostedt, A. Graf, R. Hill, S.P. Hau-Riege, J.J. Rocca, Nature 481 (2012) 488.
[6] M. Beye, S. Schreck, F. Sorgenfrei, C. Trabant, N. Pontius, C. Schüßler-Langeheine, W. Wurth, A. Föhlisch, Nature 501 (2013) 191.
[7] M. Fuchs, M. Trigo, J. Chen, S. Ghimire, S. Shwartz, M. Kozina, M. Jiang, T. Henighan, C. Bray, G. Ndabashimiye, P.H. Bucksbaum, Y. Feng, S. Herrmann, G. A. Carini, J. Pines, P. Hart, C. Kenney, S. Guillet, S. Boutet, G.J. Williams, M. Messerschmidt, M.M. Seibert, S. Moeller, J.B. Hastings, D.A. Reis, Nat. Phys. 11 (2015) 964.
[8] S. Shwartz, M. Fuchs, J.B. Hastings, Y. Inubushi, T. Ishikawa, T. Katayama, D. A. Reis, T. Sato, K. Tono, M. Yabashi, S. Yudovich, S.E. Harris, Phys. Rev. Lett. 112 (2014), 163901.
[9] R.K. Lam, S.L. Raj, T.A. Pascal, C.D. Pemmaraju, L. Foglia, A. Simoncig, N. Fabris, P. Miotti, C.J. Hull, A.M. Rizzuto, J.W. Smith, R. Mincigrucci, C. Masciovecchio, A. Gessini, E. Allaria, G. De Ninno, B. Diviacco, E. Roussel, S. Spampinati, G. Penco, S. Di Mitri, M. Trovò, M. Danailov, S.T. Christensen, D. Sokaras, T.-C.C. Weng, M. Coreno, L. Poletto, W.S. Drisdell, D. Prendergast, L. Giannessi, E. Principi, D. Nordlund, R.J. Saykally, C.P. Schwartz, Phys. Rev. Lett. 120 (2018) 23901.
[10] R.K. Lam, S.L. Raj, T.A. Pascal, C.D. Pemmaraju, L. Foglia, A. Simoncig, N. Fabris, P. Miotti, C.J. Hull, A.M. Rizzuto, J.W. Smith, R. Mincigrucci, C. Masciovecchio, A. Gessini, G. De Ninno, B. Diviacco, E. Roussel, S. Spampinati, G. Penco, S. Di Mitri, M. Trovò, M.B. Danailov, S.T. Christensen, D. Sokaras, T.C. Weng, M. Coreno, L. Poletto, W.S. Drisdell, D. Prendergast, L. Giannessi, E. Principi, D. Nordlund, R.J. Saykally, C.P. Schwartz, Chem. Phys. Lett. 703 (2018) 112.
[11] T.E. Glover, D.M. Fritz, M. Cammarata, T.K. Allison, S. Coh, J.M. Feldkamp, H. Lemke, D. Zhu, Y. Feng, R.N. Coffee, M. Fuchs, S. Ghimire, J. Chen, S. Shwartz, D.A. Reis, S.E. Harris, J.B. Hastings, Nature 488 (2012) 603.
[12] N. Bloembergen, Rev. Mod. Phys. 54 (1982) 685.
[13] K.A. Nelson, D.R. Lutz, M.D. Fayer, L. Madison, Phys. Rev. B 24 (1981) 3261.
[14] K.A. Nelson, R.J.D. Miller, D.R. Lutz, M.D. Fayer, J. Appl. Phys. 53 (1982) 1144.
[15] E.R. Warrick, A. Fidler, W. Cao, E. Bloch, D.M. Neumark, S.R. Leone, Faraday Discuss. 212 (2018) 157.
[16] W. Cao, E.R. Warrick, A. Fidler, S.R. Leone, D.M. Neumark, Phys. Rev. A 97 (2018) 1.
[17] R.I. Tobey, M.E. Siemens, O. Cohen, M.M. Murnane, H.C. Kapteyn, K.A. Nelson, Opt. Lett. 32 (2007) 286.
[18] E. Sistrunk, J. Grilj, J. Jeong, M.G. Samant, A.X. Gray, H.A. Dürr, S.S.P. Parkin, M. Gühr, Opt. Express 23 (2015) 4340.
[19] W. Cao, E.R. Warrick, A. Fidler, D.M. Neumark, S.R. Leone, Phys. Rev. A 94 (2016) 1.
[20] F. Bencivenga, R. Cucini, F. Capotondi, A. Battistoni, R. Mincigrucci, E. Giangrisostomi, A. Gessini, M. Manfredda, I.P.P. Nikolov, E. Pedersoli, E. Principi, C. Svetina, P. Parisse, F. Casolari, M.B.B. Danailov, M. Kiskinova, C. Masciovecchio, Nature 520 (2015) 205.
[21] F. Bencivenga, A. Calvi, F. Capotondi, R. Cucini, R. Mincigrucci, A. Simoncig, M. Manfredda, E. Pedersoli, E. Principi, F. Dallari, R.A.A. Duncan, M.G.G. Izzo, G. Knopp, A.A.A. Maznev, G. Monaco, S. Di Mitri, A. Gessini, L. Giannessi, N. Mahne, I.P.P. Nikolov, R. Passuello, L. Raimondi, M. Zangrando, C. Masciovecchio, Faraday Discuss. 194 (2016) 283.
[22] A.A. Maznev, F. Bencivenga, A. Cannizzo, F. Capotondi, R. Cucini, R.A. Duncan, T. Feurer, T.D. Frazer, L. Foglia, H.-M. Frey, H. Kapteyn, J. Knobloch, G. Knopp, C. Masciovecchio, R. Mincigrucci, G. Monaco, M. Murnane, I. Nikolov, E. Pedersoli, A. Simoncig, A. Vega-Flick, K.A. Nelson, Appl. Phys. Lett. 113 (2018), 221905.
[23] F. Bencivenga, C. Masciovecchio, Nucl. Instruments Methods Phys. Res. Sect. A Accel. Spectrom. Detect. Assoc. Equip. 606 (2009) 785.
[24] F. Bencivenga, et al., Sci. Adv. 5 (2019) eaaw5805.
[25] L. Foglia, F. Bencivenga, R. Mincigrucci, A. Simoncig, A. Calvi, R. Cucini, E. Principi, M. Zangrando, N. Mahne, M. Manfredda, L. Raimondi, E. Pedersoli, F. Capotondi, M. Kiskinova, C. Masciovecchio, Proc. SPIE. Int. Soc. Opt. Eng. 10237 (2017) 102370C.
[26] R. Mincigrucci, L. Foglia, D. Naumenko, E. Pedersoli, A. Simoncig, R. Cucini, A. Gessini, M. Kiskinova, G. Kurdi, N. Mahne, M. Manfredda, I.P. Nikolov, E. Principi, L. Raimondi, M. Zangrando, C. Masciovecchio, F. Capotondi, F. Bencivenga, Nucl. Instrum. Methods Phys. Res. Sect. A Accel. Spectrom. Detect. Assoc. Equip. 907 (2018) 132.
[27] F. Capotondi, L. Foglia, M. Kiskinova, C. Masciovecchio, R. Mincigrucci, D. Naumenko, E. Pedersoli, A. Simoncig, F. Bencivenga, J. Synchrotron Radiat. 25 (2018) 32.
[28] E. Allaria, R. Appio, L. Badano, W.A.A. Barletta, S. Bassanese, S.G.G. Biedron, A. Borga, E. Busetto, D. Castronovo, P. Cinquegrana, S. Cleva, D. Cocco, M. Cornacchia, P. Craievich, I. Cudin, G. D'Auria, M. Dal Forno, M.B.B. Danailov, R. De Monte, G. De Ninno, P. Delgiusto, A. Demidovich, S. Di Mitri, B. Diviacco, A. Fabris, R. Fabris, W. Fawley, M. Ferianis, E. Ferrari, S. Ferry, L. Froehlich, P. Furlan, G. Gaio, F. Gelmetti, L. Giannessi, M. Giannini, R. Gobessi, R. Ivanov, E. Karantzoulis, M. Lonza, A. Lutman, B. Mahieu, M. Milloch, S.V.V. Milton, M. Musardo, I. Nikolov, S. Noe, F. Parmigiani, G. Penco, M. Petronio, L. Pivetta, M. Predonzani, F. Rossi, L. Rumiz, A. Salom, C. Scafuri, C. Serpico, P. Sigalotti, S. Spampinati, C. Spezzani, M. Svandrlik, C. Svetina, S. Tazzari, M. Trovo, R. Umer, A. Vascotto, M. Veronese, R. Visintini, M. Zaccaria, D. Zangrando, M. Zangrando, Nat. Photonics 6 (2012) 699.
[29] E. Allaria, D. Castronovo, P. Cinquegrana, P. Craievich, M. Dal Forno, M. B. Danailov, G. D'Auria, A. Demidovich, G. De Ninno, S. Di Mitri, B. Diviacco, W. M. Fawley, M. Ferianis, E. Ferrari, L. Froehlich, G. Gaio, D. Gauthier, L. Giannessi, R. Ivanov, B. Mahieu, N. Mahne, I. Nikolov, F. Parmigiani, G. Penco, L. Raimondi, C. Scafuri, C. Serpico, P. Sigalotti, S. Spampinati, C. Spezzani, M. Svandrlik, C. Svetina, M. Trovo, M. Veronese, D. Zangrando, M. Zangrando, Nat. Photonics 7 (2013) 913.
[30] R. Cucini, F. Bencivenga, C. Masciovecchio, Opt. Lett. 36 (2011) 1032.
[31] L. Foglia, F. Capotondi, R. Mincigrucci, D. Naumenko, E. Pedersoli, A. Simoncig, G. Kurdi, A. Calvi, M. Manfredda, L. Raimondi, N. Mahne, M. Zangrando, C. Masciovecchio, F. Bencivenga, Phys. Rev. Lett. 120 (2018), 263901.
[32] F. Bencivenga, F. Capotondi, F. Casolari, F. Dallari, M.B.M.B. Danailov, G. De Ninno, D. Fausti, M. Kiskinova, M. Manfredda, C. Masciovecchio, E. Pedersoli, Faraday Discuss. 171 (2014) 487.
[33] R. Bohinc, G. Pamfilidis, J. Rehault, P. Radi, C. Milne, J. Szlachetko, F. Bencivenga, F. Capotondi, R. Cucini, L. Foglia, C. Masciovecchio, R. Mincigrucci, E. Pedersoli, A. Simoncig, N. Mahne, A. Cannizzo, H.M. Frey, Z. Ollmann, T. Feurer, A. A. Maznev, K. Nelson, G. Knopp, Appl. Phys. Lett. 114 (2019), 181101.
[34] B.D. Patterson, Slac-Tn 026 (2010).
[35] H. Kogelnik, Bell Syst. Tech. J. 48 (1969) 2909.
[36] M.G. Moharam, T.K. Gaylord, R. Magnusson, Opt. Commun. 32 (1980) 19.
[37] Robert W. Boyd, R. Boyd, Nonlinear Optics, third ed., Elsevier, 1996.
[38] E. Allaria, F. Bencivenga, R. Borghes, F. Capotondi, D. Castronovo, P. Charalambous, P. Cinquegrana, M.B.B. Danailov, G. De Ninno, A. Demidovich, S. Di Mitri, B. Diviacco, D. Fausti, W.M.M. Fawley, E. Ferrari, L. Froehlich, D. Gauthier, A. Gessini, L. Giannessi, R. Ivanov, M. Kiskinova, G. Kurdi, B. Mahieu, N. Mahne, I. Nikolov, C. Masciovecchio, E. Pedersoli, G. Penco, L. Raimondi, C. Serpico, P. Sigalotti, S. Spampinati, C. Spezzani, C. Svetina, M. Trovò, M. Zangrando, Nat. Commun. 4 (2013) 1.
[39] E. Ferrari, C. Spezzani, F. Fortuna, R. Delaunay, F. Vidal, I. Nikolov, P. Cinquegrana, B. Diviacco, D. Gauthier, G. Penco, P.R. Ribic, E. Roussel, M. Trovo, J.B. Moussy, T. Pincelli, L. Lounis, M. Manfredda, E. Pedersoli, F. Capotondi, C. Svetina, N. Mahne, M. Zangrando, L. Raimondi, A. Demidovich, L. Giannessi, G. De Ninno, M.B. Danailov, E. Allaria, M. Sacchi, Nat. Commun. 7 (2016) 1.
[40] C. Ferrante, E. Pontecorvo, G. Cerullo, A. Chiasera, G. Ruocco, W. Schirmacher, T. Scopigno, Nat. Commun. 4 (2013) 1793.
[41] F. Mallamace, C. Corsaro, H.E. Stanley, Proc. Natl. Acad. Sci. 110 (2013) 4899.
[42] M.E. Siemens, Q. Li, R. Yang, K.A. Nelson, E.H. Anderson, M.M. Murnane, H. C. Kapteyn, Nat. Mater. 9 (2010) 26.
[43] K.M. Hoogeboom-Pot, J.N. Hernandez-Charpak, X. Gu, T.D. Frazer, E.H. Anderson, W. Chao, R.W. Falcone, R. Yang, M.M. Murnane, H.C. Kapteyn, D. Nardi, Proc. Natl. Acad. Sci. 112 (2015) 4846.
[44] Y. Hu, L. Zeng, A.J. Minnich, M.S. Dresselhaus, G. Chen, Nat. Nanotechnol. 10 (2015) 701.
[45] A. Eschenlohr, M. Battiato, P. Maldonado, N. Pontius, T. Kachel, K. Holldack, R. Mitzner, A. Föhlisch, P.M. Oppeneer, C. Stamm, Nat. Mater. 12 (2013) 332.
[46] T.A. Ostler, J. Barker, R.F.L. Evans, R.W. Chantrell, U. Atxitia, O. Chubykalo-Fesenko, S. El Moussaoui, L. Le Guyader, E. Mengotti, L.J. Heyderman, F. Nolting, A. Tsukamoto, A. Itoh, D. Afanasiev, B.A. Ivanov, A.M. Kalashnikova, K. Vahaplar, J. Mentink, A. Kirilyuk, T. Rasing, A.V. Kimel, Nat. Commun. 3 (2012) 666.
[47] A. Kirilyuk, A.V. Kimel, T. Rasing, Rev. Mod. Phys. 82 (2010) 2731.
[48] G.M. Choi, B.C. Min, K.J. Lee, D.G. Cahill, Nat. Commun. 5 (2014) 1.
[49] P.G. Sverdrup, S. Sinha, M. Asheghi, S. Uma, K.E. Goodson, Appl. Phys. Lett. 78 (2001) 3331.

[50] G. Chen, Phys. Rev. Lett. 86 (2001) 2297.
[51] J.A. Johnson, A.A. Maznev, J. Cuffe, J.K. Eliason, A.J. Minnich, T. Kehoe, C.M. S. Torres, G. Chen, K.A. Nelson, Phys. Rev. Lett. 110 (2013), 025901.
[52] A.A. Maznev, J.A. Johnson, K.A. Nelson, J. Appl. Phys. 109 (2011) 1.
[53] R.C. Zeller, R.O. Pohl, Phys. Rev. B 4 (1971) 2029.
[54] S. Gelin, H. Tanaka, A. Lemaître, Nat. Mater. 15 (2016) 1177.
[55] A.I. Chumakov, G. Monaco, A. Monaco, W.A. Crichton, A. Bosak, R. Rüffer, A. Meyer, F. Kargl, L. Comez, D. Fioretto, H. Giefers, S. Roitsch, G. Wortmann, M. H. Manghnani, A. Hushur, Q. Williams, J. Balogh, K. Parliński, P. Jochym, P. Piekarz, Phys. Rev. Lett. 106 (2011) 1.
[56] G. Monaco, S. Mossa, Proc. Natl. Acad. Sci. U. S. A. 106 (2009) 16907.
[57] Y. Shvyd'Ko, S. Stoupin, D. Shu, S.P. Collins, K. Mundboth, J. Sutter, M. Tolkiehn, Y. Shvyd'ko, S. Stoupin, D. Shu, S.P. Collins, K. Mundboth, J. Sutter, M. Tolkiehn, Y. Shvyd'Ko, S. Stoupin, D. Shu, S.P. Collins, K. Mundboth, J. Sutter, M. Tolkiehn, Nat. Commun. 5 (2014) 1.
[58] S.H. Kim, D.B. Asay, M.T. Dugger, Nano Today 2 (2007) 22.
[59] L. Raimondi, C. Svetina, N. Mahne, D. Cocco, A. Abrami, M. De Marco, C. Fava, S. Gerusina, R. Gobessi, F. Capotondi, E. Pedersoli, M. Kiskinova, G. De Ninno, P. Zeitoun, G. Dovillaire, G. Lambert, W. Boutu, H. Merdji, A.I. Gonzalez, D. Gauthier, M. Zangrando, Nucl. Instrum. Methods Phys. Res. Sect. A Accel. Spectrom. Detect. Assoc. Equip. 710 (2013) 131.
[60] R. Mincigrucci, D. Naumenko, L. Foglia, I. Nikolov, E. Pedersoli, E. Principi, A. Simoncig, M. Kiskinova, C. Masciovecchio, F. Bencivenga, F. Capotondi, Opt. Express 26 (2018) 11879.
[61] S.M. Durbin, AIP Adv. 2 (2012) 42151.
[62] N. Medvedev, B. Rethfeld, New J. Phys. 1 (2010), 073037.
[63] H.J. Zeiger, J. Vidal, T.K. Cheng, E.P. Ippen, G. Dresselhaus, M.S. Dresselhaus, Phys. Rev. B 45 (1992) 768.
[64] M. Först, T. Dekorsy, C. Trappe, M. Laurenzis, H. Kurz, B. Béchevet, Appl. Phys. Lett. 77 (2000) 1964.
[65] D. Lee, S. Akturk, P. Gabolde, R. Trebino, Opt. Express 15 (2007) 760.
[66] H.J. Eichler, U. Klein, D. Langhans, Appl. Phys. 21 (1980) 215.
[67] M. Dantus, Annu. Rev. Phys. Chem. 52 (2001) 639.
[68] S. Mukamel, Y. Tanimura, P. Hamm, Acc. Chem. Res. 42 (2009) 1207.
[69] K.C. Prince, E. Allaria, C. Callegari, R. Cucini, G. De Ninno, S. Di Mitri, B. Diviacco, E. Ferrari, P. Finetti, D. Gauthier, L. Giannessi, N. Mahne, G. Penco, O. Plekan, L. Raimondi, P. Rebernik, E. Roussel, C. Svetina, M. TrovÃ, M. Zangrando, M. Negro, P. Carpeggiani, M. Reduzzi, G. Sansone, A.N. Grum-Grzhimailo, E. V. Gryzlova, S.I. Strakhova, K. Bartschat, N. Douguet, J. Venzke, D. Iablonskyi, Y. Kumagai, T. Takanashi, K. Ueda, A. Fischer, M. Coreno, F. Stienkemeier, Y. Ovcharenko, T. Mazza, M. Meyer, Nat. Photonics 10 (2016) 176.
[70] A. Fabris, E. Allaria, L. Badano, F. Bencivenga, C. Callegari, F. Capotondi, D. Castronovo, F. Cilento, P. Cinquegrana, M. Coreno, R. Cucini, I. Cudin, M. B. Danailov, G. D'Auria, R. De Monte, G. De Ninno, P. Delgiusto, A. Demidovich, S. Di Mitri, B. Diviacco, R. Fabris, W.M. Fawley, M. Ferianis, E. Ferrari, P. Finetti, P. F. Radivo, G. Gaio, D. Gauthier, F. Gelmetti, L. Giannessi, F. Iazzourene, M. Kiskinova, S. Krecic, M. Lonza, N. Mahne, M. Malvestuto, C. Masciovecchio, M. Milloch, F. Parmigiani, G. Penco, A. Perucchi, L. Pivetta, O. Plekan, M. Predonzani, E. Principi, L. Raimondi, P.R. Ribic, F. Rossi, E. Roussel, L. Rumiz, C. Scafuri, C. Serpico, P. Sigalotti, M. Svandrlik, C. Svetina, M. Trovò, A. Vascotto, M. Veronese, R. Visintini, D. Zangrando, M. Zangrando. in IPAC 2016 - Proc.7th Int. Part. Accel. Conf., 2016.
[71] Z.T. Zhao, D. Wang, J.H. Chen, Z.H. Chen, H.X. Deng, J.G. Ding, C. Feng, Q. Gu, M. M. Huang, T.H. Lan, Y.B. Leng, D.G. Li, G.Q. Lin, B. Liu, E. Prat, X.T. Wang, Z. S. Wang, K.R. Ye, L.Y. Yu, H.O. Zhang, J.Q. Zhang, M. Zhang, M. Zhang, T. Zhang, S.P. Zhong, Q.G. Zhou, Nat. Photonics 6 (2012) 360.